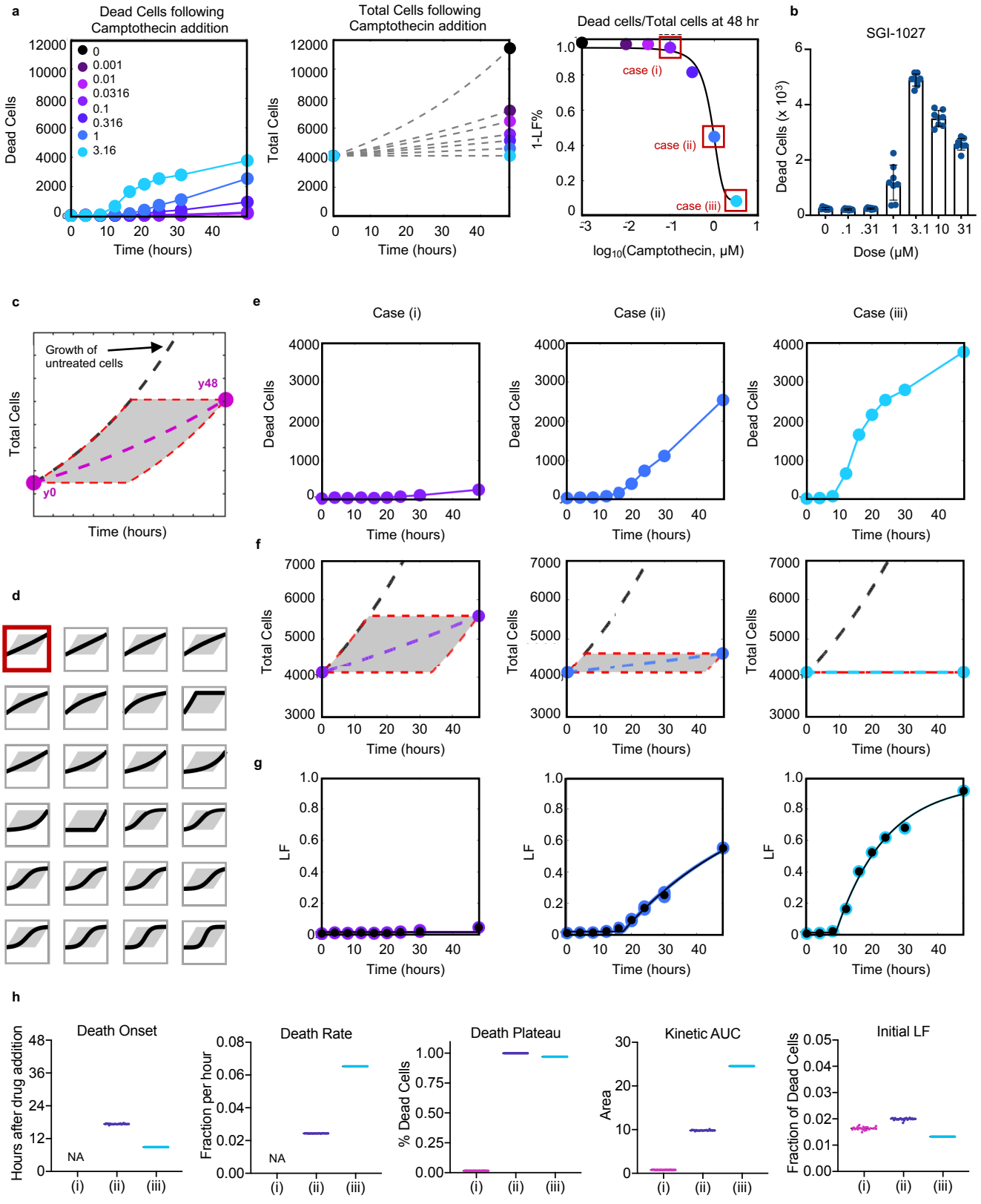

Supplementary Figure 1 – Estimation of lethal fraction dynamics over time using a plate reader based SYTOX assay. (a) Experimental measurement of dead cells over time (left) and total cells at the beginning and end of the assay (middle). These numbers can be used to determine the lethal fraction (LF%) at the assay end point (right), without the use of any computationally inferred values. Data shown as an example are for camptothecin at 7 doses (half-log dilution, as in this study). Three doses representing cases (i-iii), highlighted in panels e-h, represent non-lethal doses (i), intermediate killing doses (ii), and strong killing doses (iii). Legend continued on next page.

Supplementary Figure 1 – Estimation of lethal fraction dynamics over time using a plate reader based SYTOX assay. Continued from previous. (**b**) Dead cell number is an unreliable surrogate for LF%. SGI-1027 shown as an example, in which all doses greater than 3 μM induce ~ 100% LF. Data are mean +/- SD (n = 8). **(c)** Estimating population growth kinetics in drug treated cells. To facilitate LF% calculation at intermediate time points during the assay, the kinetics of population growth must be estimated to generate a number for total cells (live cells + dead cells), which is the denominator in a LF calculation. In this study we estimated growth kinetics using an exponential model (purple dotted line). Grey area represents a region of ambiguity for the population growth model, with upper and lower bounds set by the initial population size (y0) and observed population size at the end of the assay (y48). Left and right bounds shown are based on the growth rate of untreated cells (i.e. the population can cease growth, grow slowly, or grow at non-uniform rates over time, but are unlikely to grow much faster than untreated cells). **(d)** 24 population growth models tested. Red box highlights the exponential growth model used in this study. Other models tested include linear, various sigmoidal models, and models with non-uniform rates over time. Collectively these cover the entire range of ambiguity highlighted in panel (c). **(e-g)** Case studies based on the camptothecin data shown in panel (a) for a dose that induces some growth slowing but does not kill cells (case (i)); a dose induces growth slowing and kills an intermediate fraction of cells (case (ii)); a dose that induces full growth suppression and high levels of cell death (case (iii)). **(e)** Experimental measurements of dead cell numbers over time for cases (i-iii). **(f)** Regions of ambiguity as in panel (c) for cases (i-iii). **(g)** Lethal fraction kinetics calculated for each of 24 estimated growth models shown in panel (d). Exponential model with uniform growth rate shown in black. **(h)** Kinetic parameters for each case (i-iii), calculated using 24 different estimated growth models. Variations in the estimated growth model do not significantly alter death kinetics within the bounds shown in panel c.

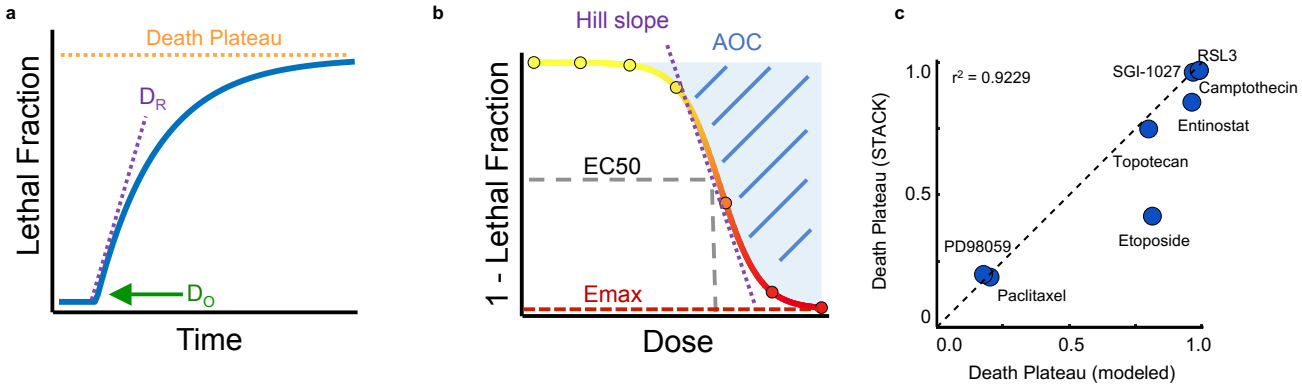

Supplementary Figure 2 – Experimental validation of plate reader based STYOX death assay. (a-b) Definitions of the kinetic (a) and pharmacometrics (b) used in this study. **(c)** Comparison between LF_{max} determined using STACK or computed using computationally inferred kinetic data. Note: D_O and D_R comparisons are shown in Fig. 2. Pharmacological response measures (EC50, Emax, hill slope, and AOC) are computed from experimental measurements without any computational inference.

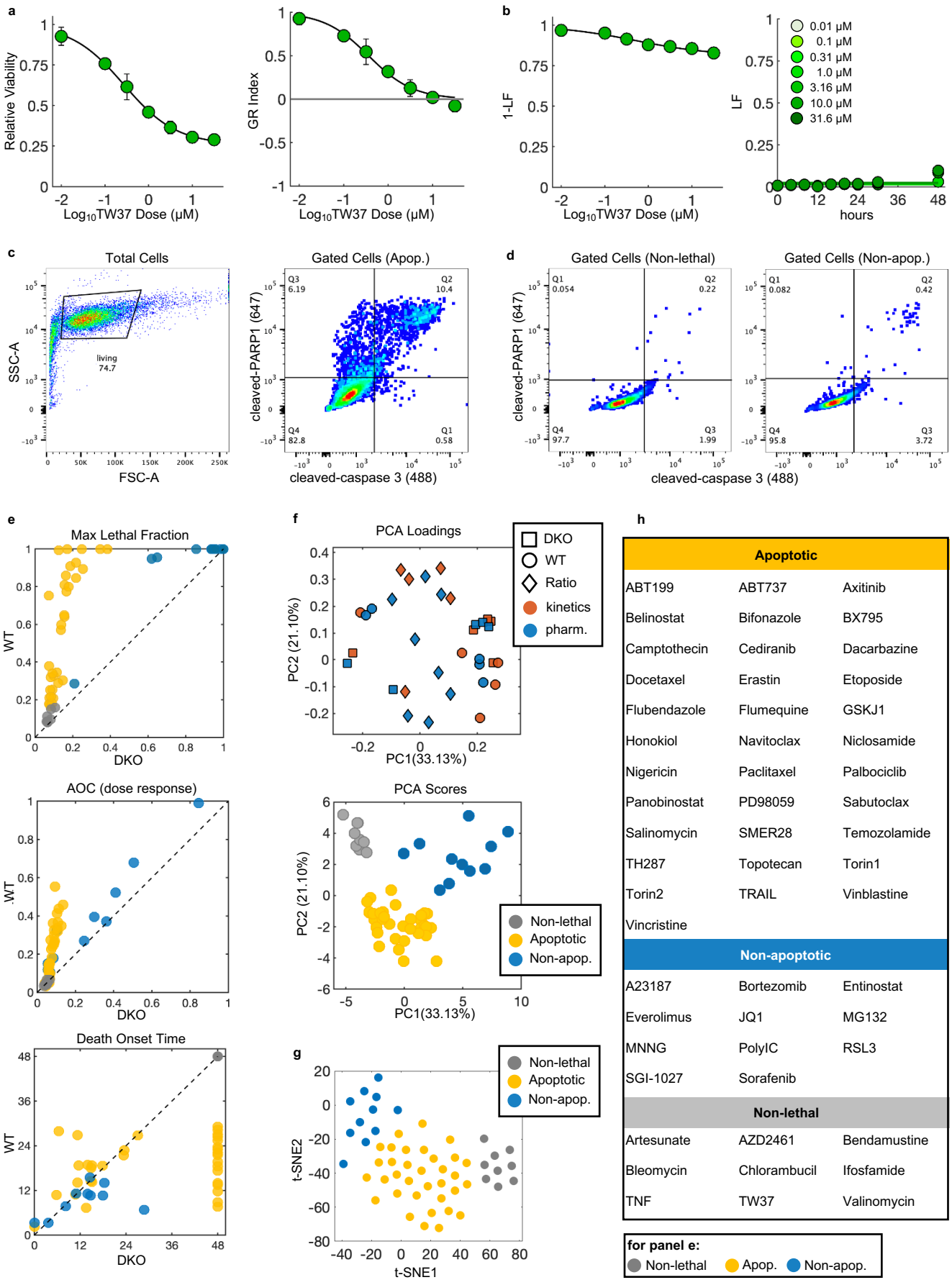

Supplementary Figure 3 – legend on next page

Supplementary Figure 3 – Evaluation of drug mechanism of killing. (a-b) Example of a non-lethal drug, TW37, which is nominally annotated as a BCL2 inhibitor. **(a)** TW37 dose response profile as measured using "relative viability" (*left*) or GR adjusted relative viability (*right*). Relative viability defined here as live cells in drug treated condition, divided by live cells in the vehicle control condition. **(b)** TW37 response calculated using lethal fraction (LF; defined here as % of dead cells within a population). 1-LF (*left*) and LF kinetics (*right*) both show lack of drug-induced increase in cell death. **(c-d)** Flow cytometry gating strategy for scoring apoptotic cells (cleaved caspase-3, cleaved PARP1 double positive cells). **(c)** 3.16 μM camptothecin shown as an example of an apoptotic drug response. **(d)** Examples of a non-lethal drug response (10 μM TW37) and a non-apoptotic drug response (10 μM MNNG). **(e-h)** Drug class determination by kinetic and pharmacological response comparison in WT and BAX/BAK$^{-/-}$ (DKO) U2OS cells. **(e)** Correlation of responses between WT and DKO cells for maximum LF (*top*), pharmacological AOC (*mid*), and death onset time (*bottom*). Grey – non-lethal compounds; Blue – non-apoptotic compounds; Gold – apoptotic compounds. **(f)** Principal component analysis of pharmacological and kinetic parameters in WT and DKO U2OS cells. Projection of observations on PC 1 and 2. Projection of loading coefficients for each parameter (*top*) and drug scores (*bottom*). Drugs colored as in (e). **(g)** t-SNE based analysis of pharmacological and kinetic data as in (f). Data in (f-g) are based on 4 biological replicates. **(h)** Drug classifications. Data in (a-b) are mean +/- SD of 4 biological replicates.

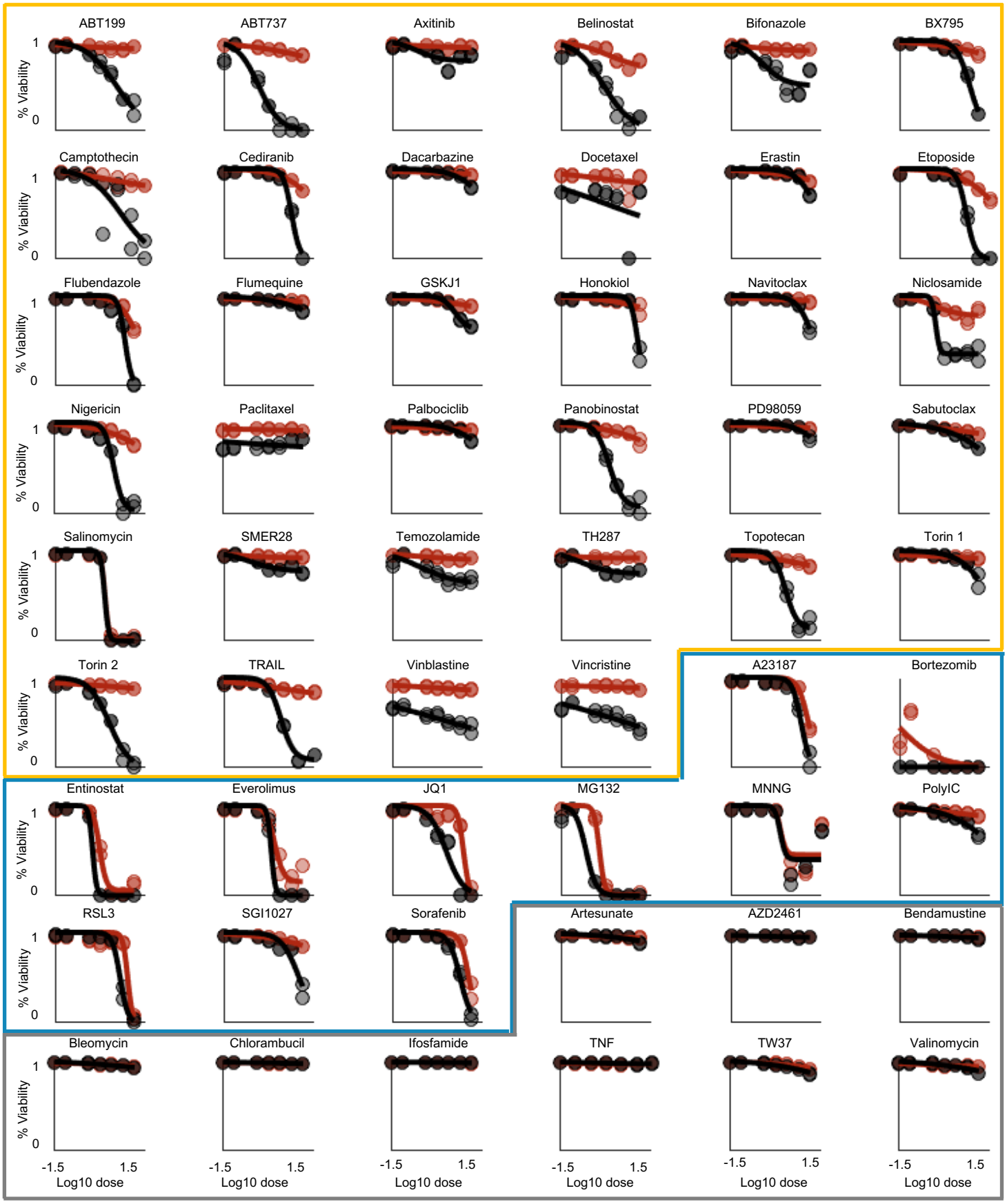

Supplementary Figure 4 – Pharmacological evaluation of drug response. Cell viability (1-LF%) of the 54 drugs used in the cell death screen in WT U2OS (black) and BAX/BAK-/- DKO cells (red). Drugs are grouped according to class (Gold area – apoptotic; Blue area – non-apoptotic; Grey area – non-lethal).

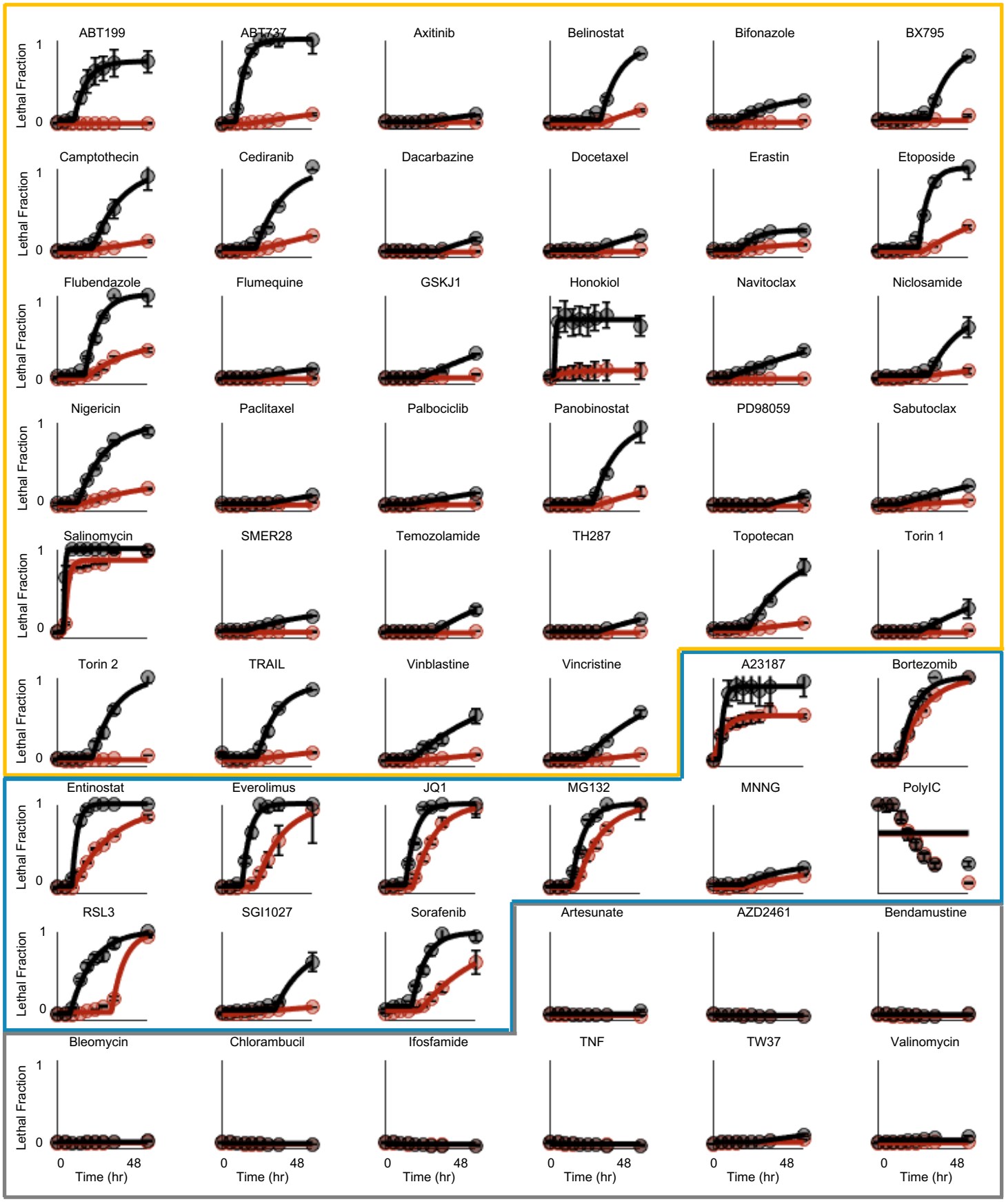

Supplementary Figure 5 – Kinetic evaluation of drug response . Lethal fraction kinetics in WT U2OS (black) and BAX/BAK$^{-/-}$ DKO (red) cell lines. Data points are mean +/- SD of 4 biological replicates. Solid lines are LED model fits. Drugs are grouped according to class (Gold area – apoptotic; Blue area – non-apoptotic; Grey area – non-lethal).

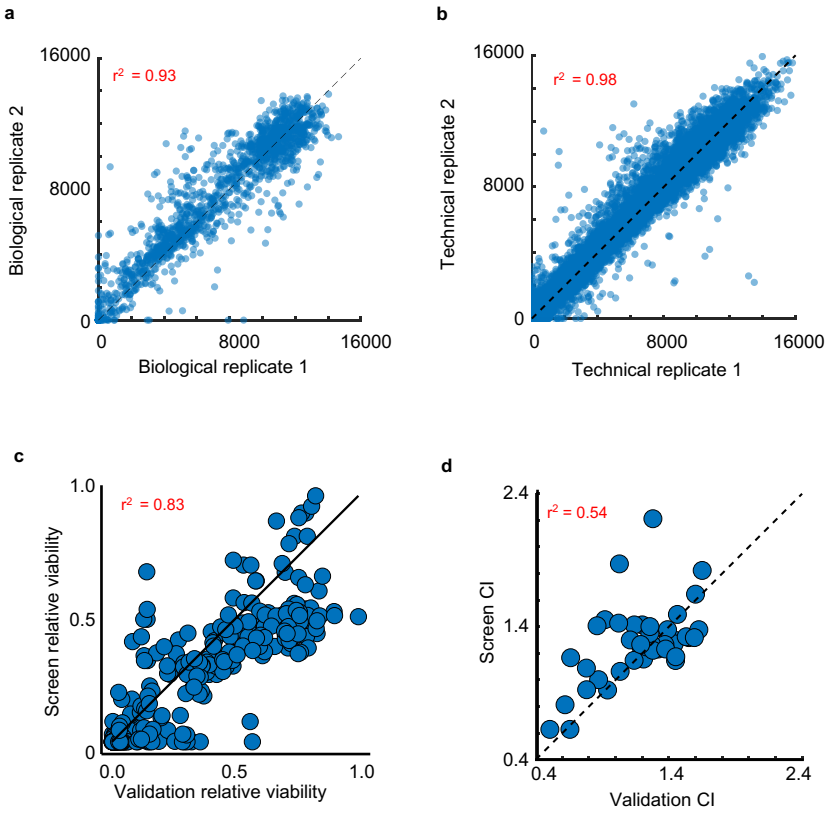

Supplementary Figure 6 – Validation of combination drug screen (a) Density plot of biological replicates (drugs tested on different days; n = 4) from the drug combination screen. Pearson correlation coefficient shown. **(b)** Density plot of "technical" replicates (drugs tested in different wells/plates but on the same day ; n = 2) from the drug combination screen. Pearson correlation coefficient shown. **(c)** Comparison of relative viability between the cell-death screen and validation experiments as measured using Cell Titer Glo. Relative viability is compared here as lethal fraction cannot be determined using Cell Titer Glo (and most other drug response assays). Data are mean values from biological replicates (n = 4). **(d)** Comparison of drug-drug interaction scores from the cell death screen measured by SYTOX and from CellTiter-Glo in validation experiments for CI. Data are mean values from biological replicates (n = 4).

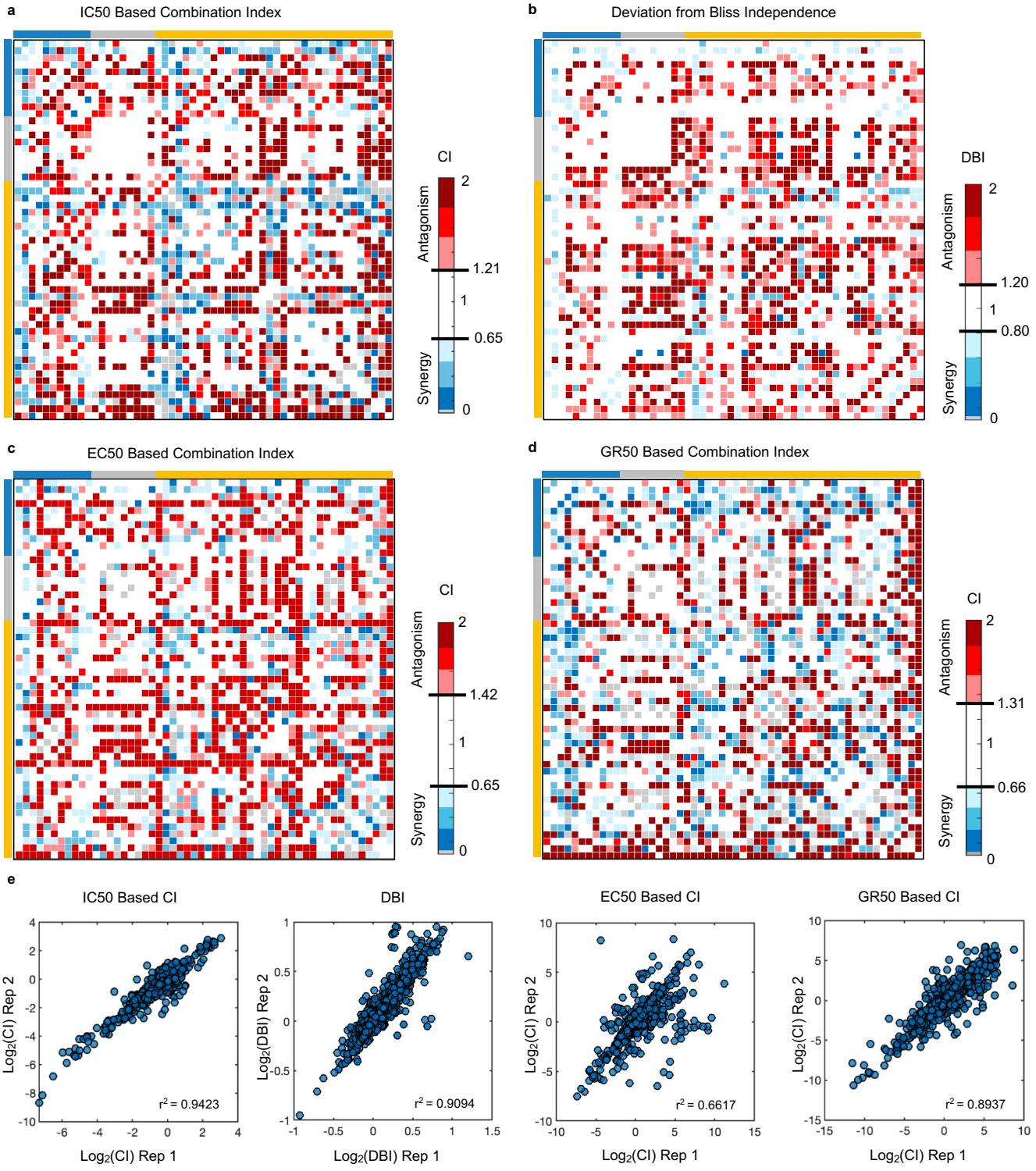

Supplementary Figure 7 – Evaluation of non-additive drug-drug interactions using different reference models and scoring conventions. (a-d) Heatmaps of drug-drug interaction scores colored according to experimentally determined thresholds for synergy and antagonism. Drug grouped by class and ordered as in Figure 3d. **(a)** Chou-Talalay Combination Index (CI) based on IC50s from 1-LF data. **(b)** Deviation from Bliss Independence based on AOC of 1-LF data. **(c)** CI computed using EC50 of 1-LF. **(d)** CI computed using GR50 transformed relative viability data. Notably for those based on 1-LF data (a-c), all scoring conventions are enriched for antagonistic drug-drug interactions. GR50 based data (d) still produce a high degree of antagonism but much higher rates of drug synergy. Among these data, GR50 is unique in that the response is strictly related to growth arrest rather than degree of cell death as in (a-c). **(e)** Drug-drug interaction scores computed separately for biological replicates. Correlation coefficient shown. Data are mean values from biological replicates (n = 4).

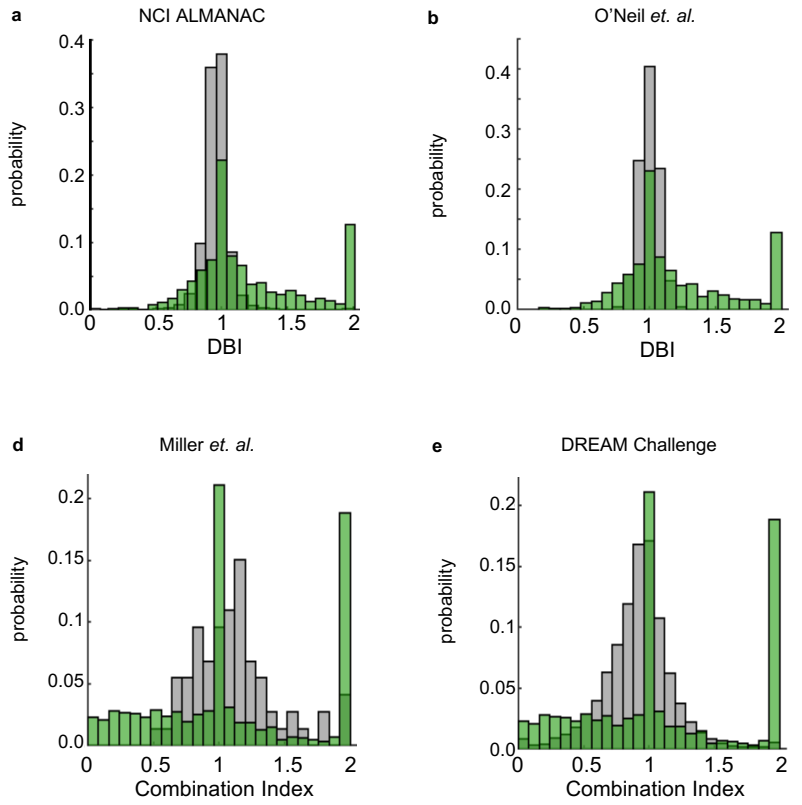

c

	Cell Death	ALMANAC	O'Neil et al.
Antag. (DBI)	35.6	1.5	2.3
Synergy (DBI)	11.0	3.8	4.4
Independent	53.4	94.7	93.3

f

	Cell Death	AZ-DREAM	Miller et al.
Antag. (CI)	30.2	10.0	9.9
Synergy (CI)	23.2	27.0	9.9
Additive	46.6	63.0	80.2

Supplementary Figure 8 – Comparison of the prevalence of non-additive drug-drug interactions within cell death drug screen compared to other combination drug screens. (a-b) Histogram of drug-drug interaction scores computed relative to a Bliss Independence reference model, comparing interactions among cell death drugs to **(a)** NCI ALMANAC, **(b)** random oncology set from ONeil et al. For each: Green – Cell death screen; Grey – Other. **(c)** Summary statistics for antagonism, synergy, and independence for drug combination screens that score relative to a Bliss reference model. **(d-e)** Histogram of drug-drug interaction scores computed relative to dose additivity reference model, comparing interactions among cell death drugs to **(d)** kinase inhibitor combinations from Miller et al. and **(e)** AZ-Dream Dataset. Colors are as in (a-b). **(f)** Summary statistics for antagonism, synergy, and additivity for drug combination screens that score relative to a dose additivity reference model.

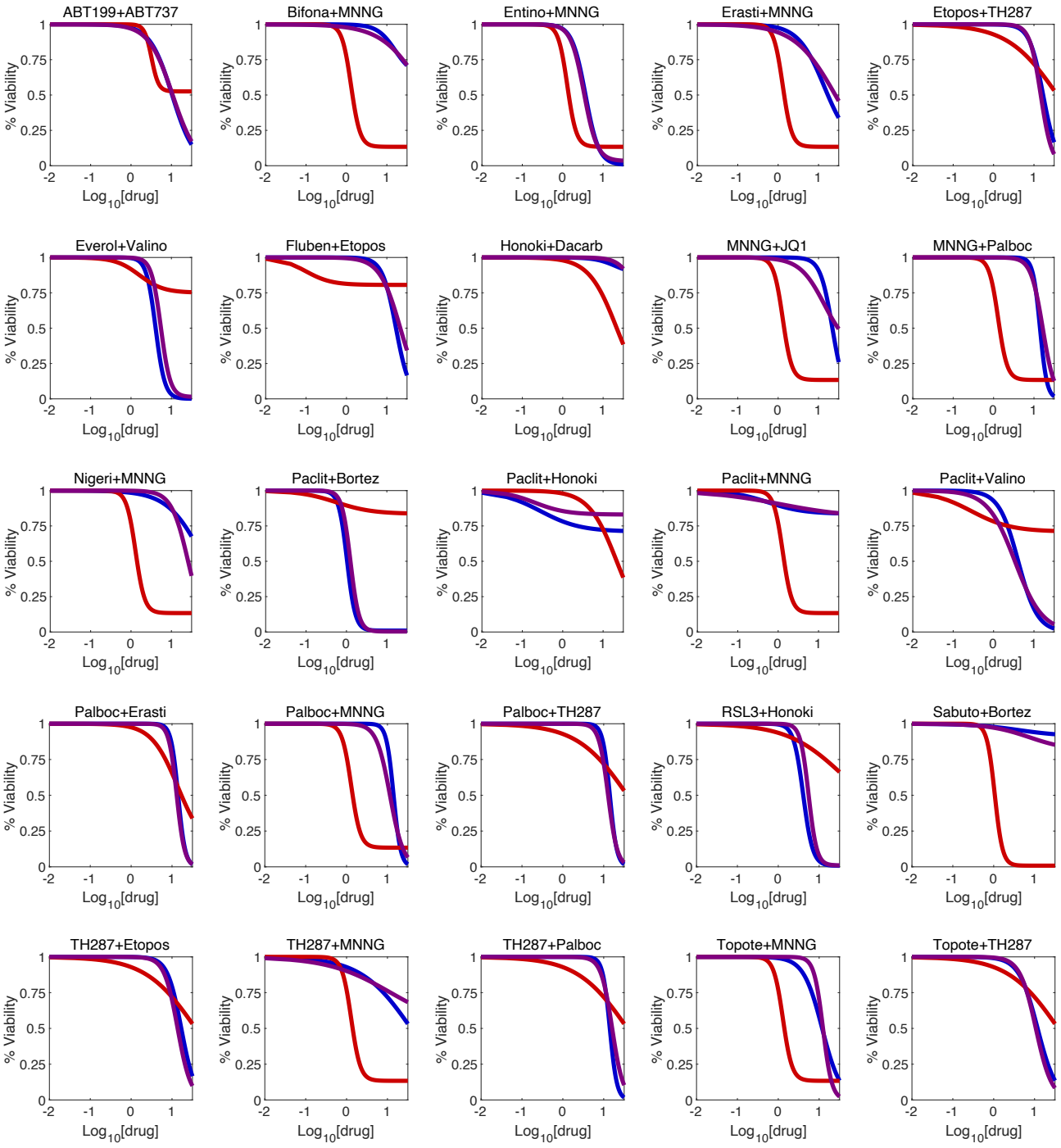

Supplementary Figure 9 – SAD combinations in U2OS cells. Example of SAD combinations. See also Supplementary Dataset 4.

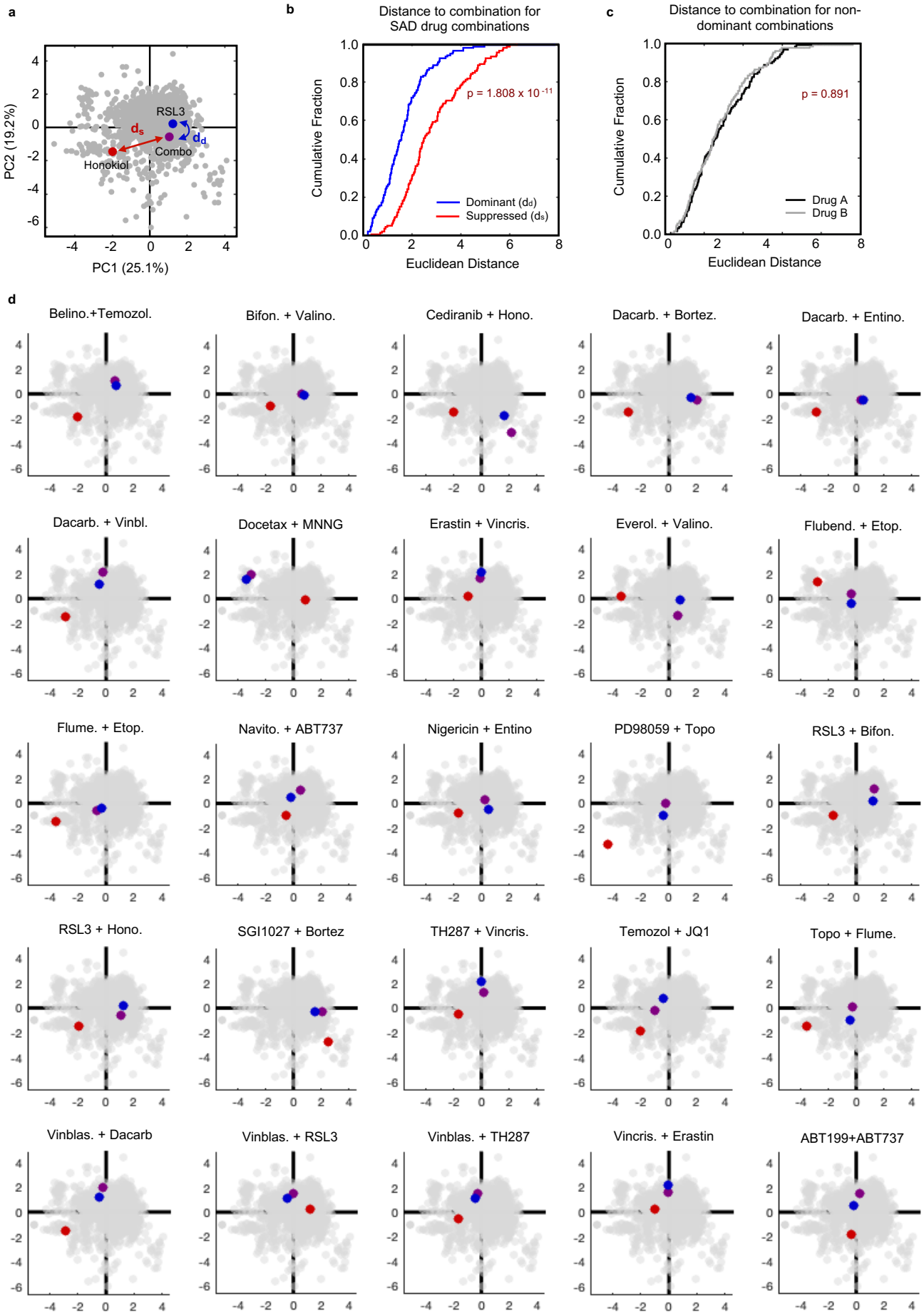

Supplementary Figure 10 – Statistical validation of drug dominance. Legend on next page.

Supplementary Figure 10 – Statistical validation of drug dominance. (a-c) Dominant drugs project closer to the drug combination than the suppressed drug in PCA space. **(a)** Example of the relative distances between a dominant (RSL3) or suppressed (Honokiol) drug and the observed SAD combination (Combo). All other combinations and single drug projections are colored grey. Note: distance to dominant drug (d_d) is shown with a curved arrow due to space limitations between the dominant and combo responses. Data in PCA are from the combination drug screen and projection shown represents the mean of biological replicates (n = 4). **(b-c)** The Euclidean distance between single drugs and their combination determined along PC's 1-3 for SAD combinations (n = 130) (b) or combinations that do not feature SAD (n = 1301). (c). p-value shown from a two-tailed KS test. **(d)** Spatial relationship between dominant drug (blue), suppressed drug (red), and SAD combination (purple) on PC's 1 and 2 for 25 of the 130 SAD combinations.

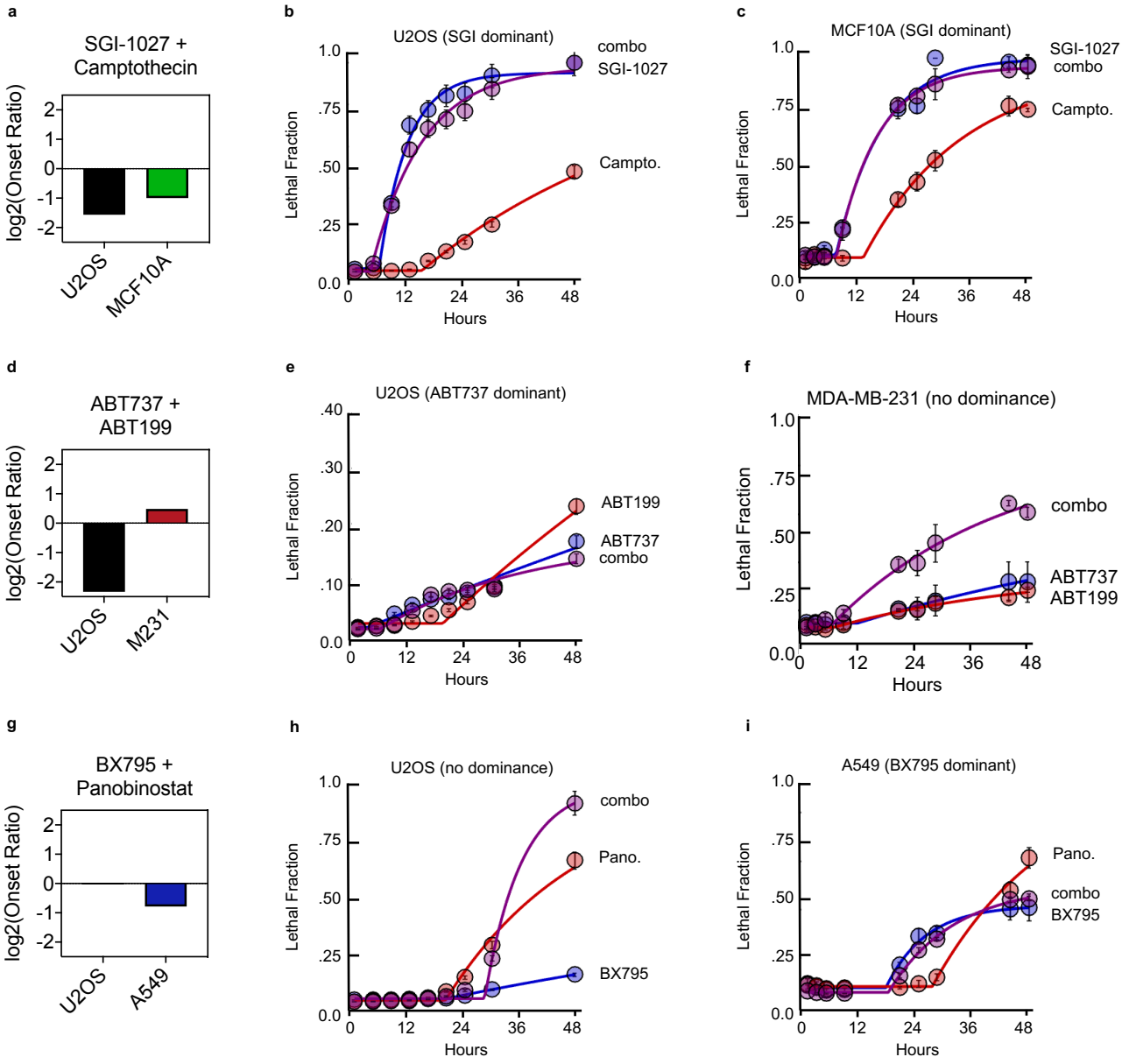

Supplementary Figure 11 – Drug dominance is associated with death onset time asymmetry across multiple cell types. (a-c) Drug combination with conserved onset time asymmetry and conserved single agent dominance in multiple cell lines. **(a)** Ratio of death onset times for SGI-1027 vs. camptothecin in U2OS and MCF10A. **(b-c)** Death kinetics in U2OS cells (b) or MCF10A cells (c) treated with SGI-1027, camptothecin, or a combination of these drugs. Both drugs used at 10 μM in both cell lines. **(d-f)** Drug combination in which onset time asymmetry and single agent dominance in U2OS cells are not observed in other cell types. **(d)** Ratio of death onset times for ABT737 vs. ABT199 in U2OS and MDA-MB-231 (M231). **(e-f)** Death kinetics in U2OS cells (e) or M231 cells (f) treated with ABT737, ABT199, or a combination of these drugs. Both drugs used at 3.16 μM in U2OS and 10 μM in M231. **(g-i)** Single agent dominance which was not observed in U2OS cells, but found in other contexts due to different onset times. **(g)** Ratio of death onset times for BX795 vs. panobinostat (Pano.) in U2OS and A549. **(h-i)** Death kinetics in U2OS cells (h) or A549 cells (i) treated with BX795, Pano., or a combination of these drugs. Both drugs used at 3.16 μM in U2OS, and 31.6 μM in A549. Data are mean +/- SD of biological replicates (n = 4).

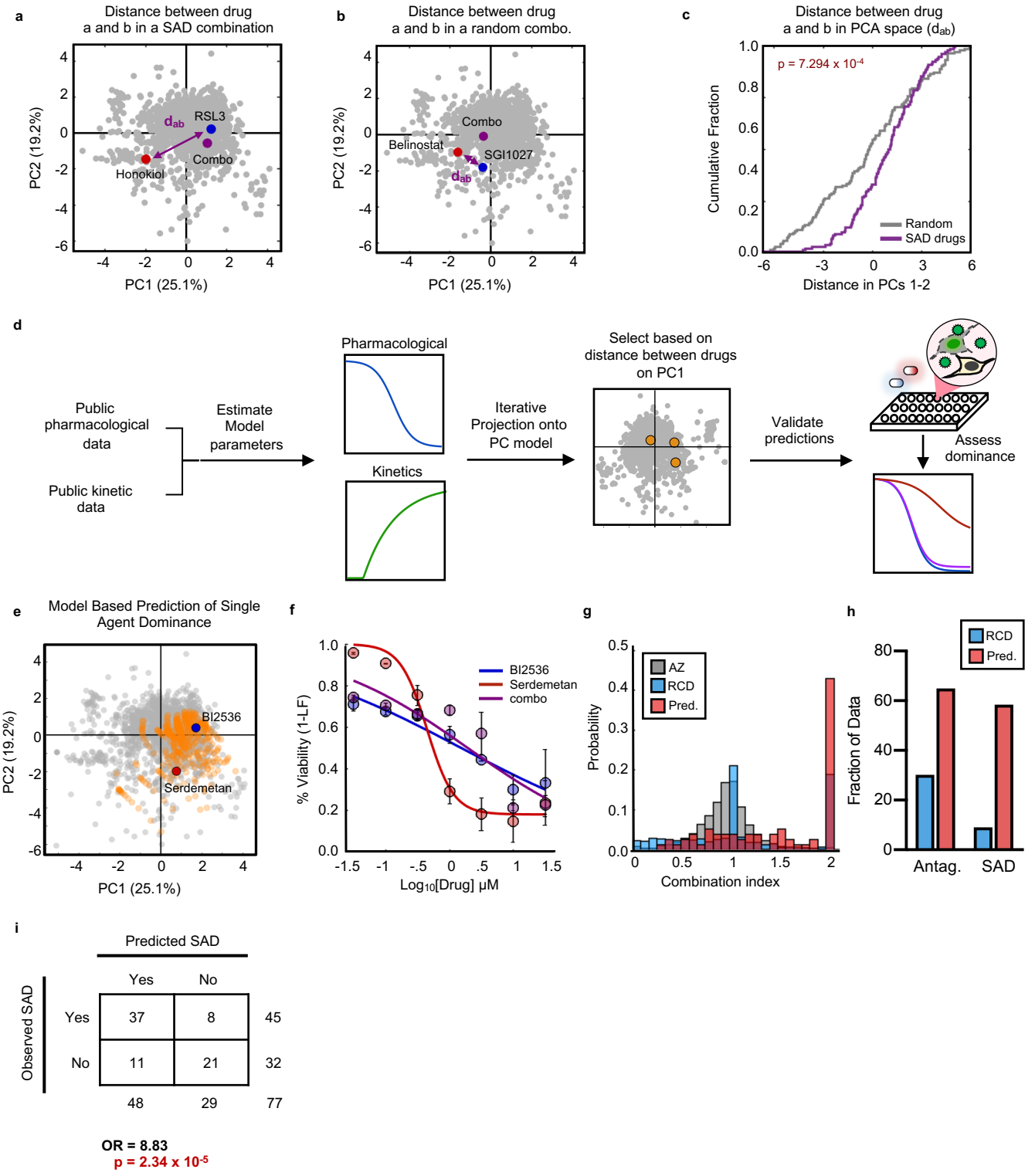

Supplementary Figure 12 – Death activation rate-based classification accurately predicts SAD combinations featuring previously untested drugs. **(a-b)** Distance between drugs a and b (d_{ab}) for a known SAD combination (a) or a non-SAD combination (b). Data in PCA are from the combination drug screen and projection shown represents the mean of biological replicates (n = 4). **(c)** Euclidean distance between a and b calculated for each drug combination (n = 130). P-value from two-tailed KS test shown. **(d)** Workflow to predict new SAD combinations. Public data were used to estimate model parameters for pharmacological and kinetic data and single drugs were projected iteratively onto the PCA model. Based on directional distance on PC1 and 2, drug combinations were classified as being putative SAD or non-SAD. Combinations were validated for antagonism and SAD using SYTOX. Legend continued on next page.

Supplementary Figure 12 – Death activation rate-based classification accurately predicts SAD combinations featuring previously untested drugs. Continued from previous. **(e)** Example of an estimated drug projection onto the PCA model. Publicly available data were used to create a probabilistic array of projections for each single drug (red and blue). All probabilistic projections are shown in orange. A single predicted SAD combination shown, with BI2536 predicted to dominate Serdemetan. Data in PCA are from the combination drug screen and projection shown represents the mean of biological replicates (n = 4). **(f)** Validation of a predicted SAD combination. Percent viability was measured by SYTOX and assessed for antagonism and SAD. Blue – BI2536 (predicted dominant); Red – Serdemetan (predicted suppressed); purple – combination. Data are mean +/- SD (n=4). **(g)** Histogram of combination indices for all 77 combinations in the model validation set. Distribution of data from the AZ-DREAM Challenge (AZ, grey), Cell Death screen (RCD, blue), and predicted SAD combinations (Pred., red). **(h-i)** Summary statistics from predictive modeling. **(h)** Percentages of antagonistic and SAD combinations. **(i)** Fisher's exact test. Odds Ratio (OR) and p-value shown for a one-sided Fisher's exact test.

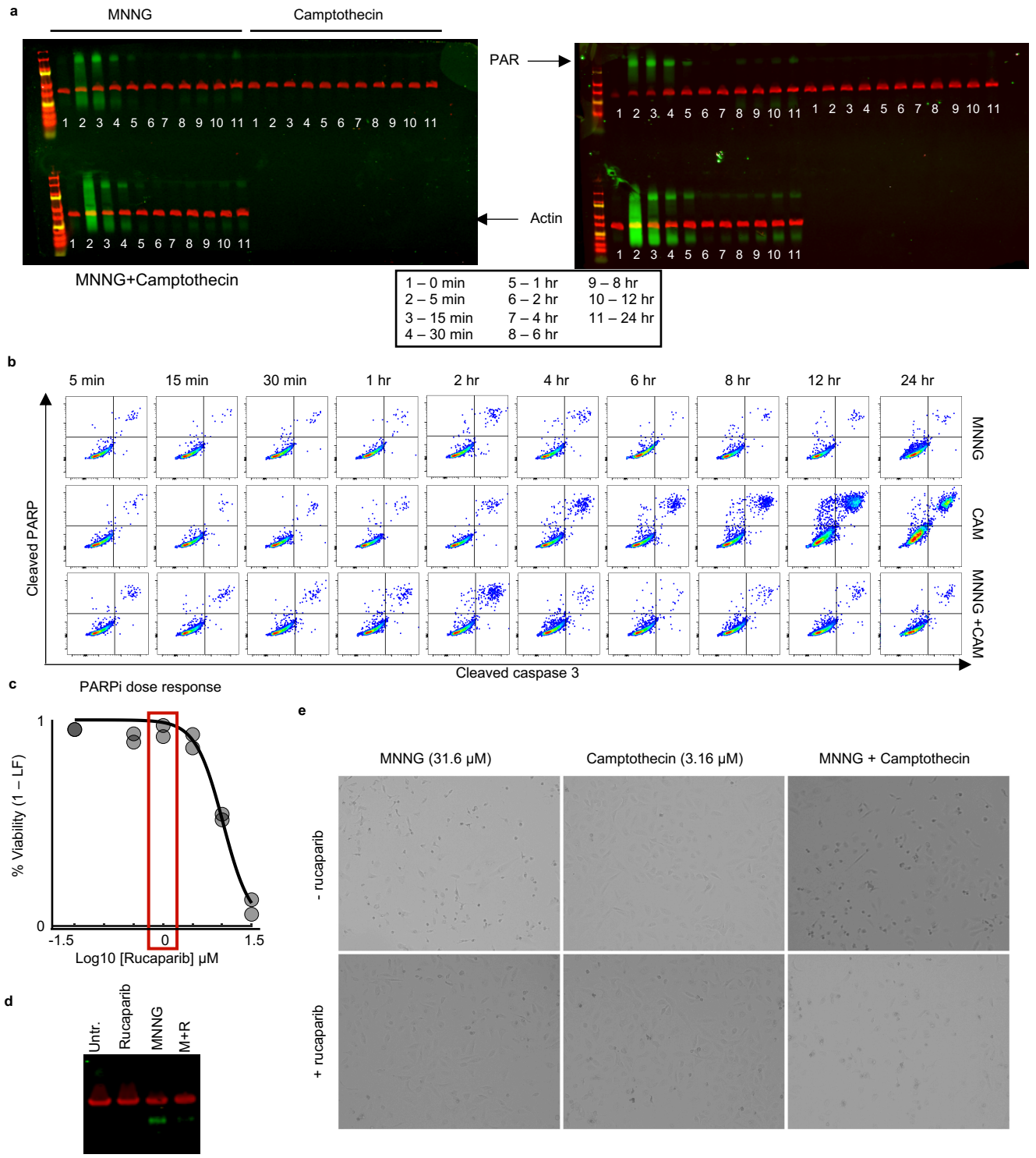

Supplementary Figure 13 – Validation of parthanatotic death induced by MNNG. **(a)** Western blot of total protein PARylation. Time course of PAR levels following treatment with MNNG, Camptothecin, or MNNG+Camptopthecin. Blots are biological replicates and time points are identical for each treatment condition. Green – PARylation; Red – β-actin. **(b)** Cleaved PARP activity over time. Representative FACS plots used to quantify cleaved PARP over time (See also Fig. 5b). **(c)** Rucaparib dose response. Rucaparib efficacy was quantified by SYTOX. A sub-lethal dose (1 μM, highlighted red) was chosen for subsequent experiments for PARP inhibition. **(d)** PAR activity in the presence of PARP inhibition. U2OS cells were treated with 1 μM rucaparib, 100 μM MNNG, or the combination for 24 hours. **(e)** Parthanatotic cell morphology. Trans illumination images of U2OS cells following indicated treatments +/- 1 μM Rucaparib at 48 hours. For panels (a,b,d and e) data are representative of 4 independent biological replicates which produced similar results.

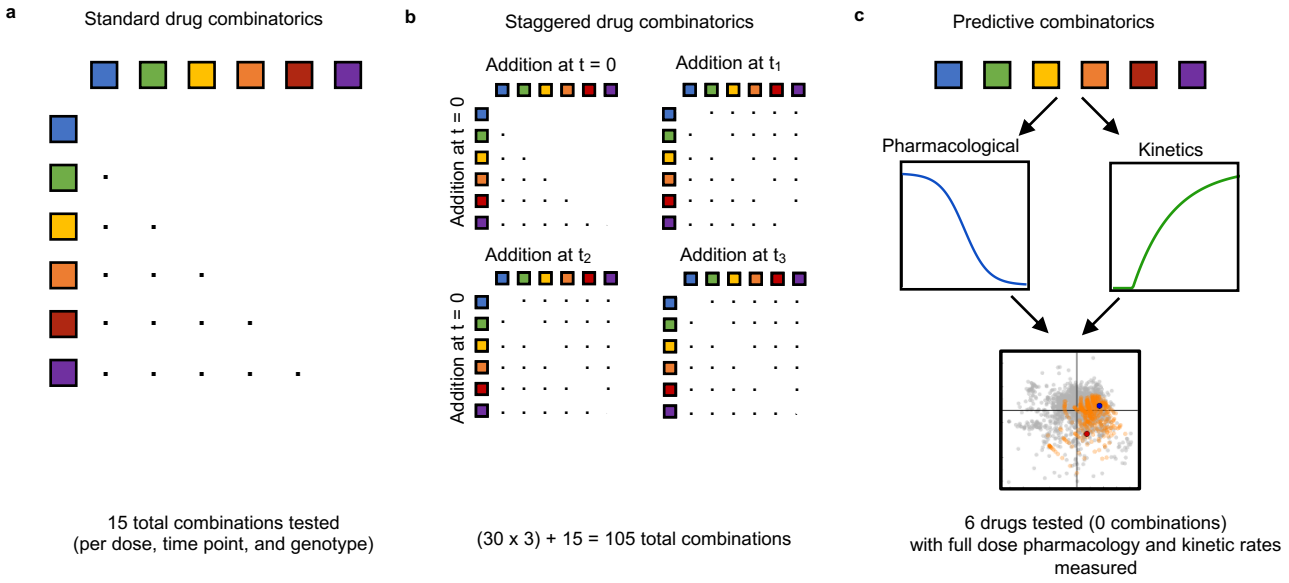

Supplementary Figure 14 – Rate-based evaluation of single drugs may improve issues related to combinatorial expansion associated with testing drug combinations. (a) Drug combinations when drugs are added at the same time. Example of testing all pairwise combinations of drugs, given that the order of drug addition does not matter. These data are for a single dose, a single dose ratio, evaluated at a single time point, in a single genetic background. **(b)** Drug combinations when relative timing of drug addition needs to be controlled. In example shown, drug "A" is added at t = 0 and drug "B" is added at time t_i. Total combinations shown for 3 temporal staggers, again at a single dose, single dose-ratio, single time point, and in a single genetic background. **(c)** Predictive combinations using a rate-based classifier. Using predictive models, testing drugs in combination may not be necessary. For instance, to identifying and avoiding SAD combinations, drugs can be tested only individually. Single drug kinetics and pharmacological parameters are then measured and modeled using PCA to predict antagonistic interactions, and the optimal drug temporal regimen needed to avoid SAD combinations in favor of response additivity.

Supplementary Table 1. Combination drug screen summary statistics

Method	Ant Threshold	Syn Threshold	Number of antagonisms	Number of Synergies	% Antagonism	%Synergy
CI (IC50)	**1.21**	**0.65**	**432**	**332**	**30.2**	**23.2**
DBI (AOC)	**1.2**	**0.8**	**509**	**158**	**35.6**	**11.0**
CI (EC50)	1.42	0.65	473	338	33.1	23.6
CI (GR50)	1.31	0.66	413	470	28.9	32.8
CI (IC70)	1.21	0.65	377	316	26.4	22.1
				average	**30.8**	**22.6**

Supplementary Table 2. Chemical list

Chemical	Source	Purity	Catalogue Number
PD98059	Apex Biologics	>98%	A1663
Vincristine	Apex Biologics	98%	A1765
Cediranib (AZD217)	Apex Biologics	98%	A1882
Bromodomain Inhibitor, (+)-JQ1	Apex Biologics	>98%	A1910
Bendamustine HCl	Apex Biologics	98%	A1984
Ifosfamide	Apex Biologics	98.65%	A2097
Dacarbazine	Apex Biologics	99.89%	A2197
MG-132	Apex Biologics	98%	A2585
Bortezomib (PS-341)	Apex Biologics	>96%	A2614
ABT-263 (Navitoclax)	Apex Biologics	>98%	A3007
Sorafenib	Apex Biologics	99.89%	A3009
Vinblastine sulfate	Apex Biologics	98.26	A3920
Belinostat (PXD101)	Apex Biologics	>98%	A4096
AZD2461	Apex Biologics	98%	A4164
GSK J1	Apex Biologics	98%	A4191
Sabutoclax	Apex Biologics	98%	A4199
TW-37	Apex Biologics	99.12%	A4234
Paclitaxel (Taxol)	ApexBio Technology	>98%	A4393
Docetaxel	ApexBio Technology	>98%	A4394
Everolimus (RAD001)	ApexBio Technology	>98%	A8169
Entinostat (MS-275,SNDX-275)	ApexBio Technology	>98%	A8171
Panobinostat (LBH589)	ApexBio Technology	>98%	A8178
ABT-737	ApexBio Technology	>95%	A8193
ABT-199	ApexBio Technology	>98%	A8194
BX795	ApexBio Technology	>94%	A8222
Torin 1	ApexBio Technology	>98%	A8312
PD 0332991 (Palbociclib) HCl	ApexBio Technology	>98%	A8316
Bleomycin Sulfate	ApexBio Technology	>98%	A8331
Axitinib (AG 013736)	ApexBio Technology	>99%	A8370
Temozolomide	ApexBio Technology	99.62%	B1399
SGI-1027	ApexBio Technology	98.59%	B1622
Torin 2	ApexBio Technology	99.37	B1640
Flubendazole	ApexBio Technology	>98%	B1759
Bifonazole	ApexBio Technology	>98%	B1897
Niclosamide	ApexBio Technology	>98%	B2283
Flumequine	ApexBio Technology	>98%	B2292
Topotecan HCl	ApexBio Technology	>99%	B2296
Artesunate	ApexBio Technology	>98%	B3662
Chlorambucil	ApexBio Technology	>98%	B3716
Poly(I:C)	ApexBio Technology	98%	B5551

TH287	ApexBio Technology	>98%	B5849
RSL3	ApexBio Technology	>98%	B6095
A23187	ApexBio Technology	98%	B6646
Valinomycin	Millipore-sigma	> 98%	V0627
SMER 28	Selleck Chemicals	>99%	S8240
Nigericin sodium salt	ApexBio Technology	98%	B7644
Honokiol	ApexBio Technology	>98%	N1672
Etoposide	Selleck Chemicals	>98%	S1225
Camptothecin	Selleck Chemicals	>98%	S1288
MNNG	TCI	>95%	M0527
Erastin	Selleck Chemicals	>99%	S7242
SLO	Millipore-sigma	>95%	SAE0089
TRAIL	R&D systems	>97%	375-TL-010
TNF alpha	R&D systems	>97%	210-TA
Alexa Fluor® 647 Mouse anti-Cleaved PARP (Asp 214)	BD Bioscience	NA	558710
Purified Rabbit Anti- Active Caspase-3	BD Bioscience	NA	559565
SYTOX green - 5mM solution in DMSO	ThermoFisher	NA	s7020
Cleaved-PARP (Asp214) (E2T4K) Mouse mAb	Cell Signaling Technology	Na	32563S
Goat anti-Rabbit IgG (H+L) Cross-Adsorbed Secondary Antibody, Alexa Fluor 488	ThermoFisher (invitrogen)	NA	A-11008
IRDye® 800CW Goat anti-Mouse IgG Secondary Antibody	LI-COR	NA	926-32210
IRDye® 680RD Goat anti-Rabbit IgG Secondary Antibody	LI-COR		926-68071

Supplementary Table 3. Small molecule screening data

Category	Parameter	Description
Assay	Type of assay	In vitro cell-based
	Target	Cell death pathways
	Primary measurement	Detection of cell death using SYTOX green reagent
	Key reagents	See chemical reagent table
	Assay protocol	“Drug Combination Screen” in manuscript
	Additional comments	
Library	Library size	54 compounds
	Library composition	Cell death inducing agents/apoptotic stimuli
	Source	ApexBio Technologies, Selleck chemicals, Millipore-Sigma, R&D systems
	Additional comments	
Screen	Format	384-well plates
	Concentration(s) tested	0.01 uM – 316 uM for all compounds; equivalent volume of DMSO as vehicle control
	Plate controls	DMSO
	Reagent/ compound dispensing system	12 channel pipette; 96 head Integra ViaFlo electronic pipettor
	Detection instrument and software	Tecan M1000 plate reader;Tecan iControl software suite
	Assay validation/QC	R^2 technical replicates = 0.98; r^2 biological replicates = 0.93
	Correction factors	
	Normalization	Lethal fraction measurements normalized to total cell number within a well. Relative viability normalized to DMSO controls
	Additional comments	
Post-HTS analysis	Hit criteria	Validation of antagonism and SAD phenotype
	Hit rate	~70%
	Additional assay(s)	Cell-Titer Glo; Fluorescence microscopy
	Confirmation of hit purity and structure	N/A
	Additional comments	Screen data made available

Supplementary Dataset 1 – Drug responses in U2OS WT and DKO cells. For the 54 drugs in this study, a list of nominal drug targets, drug classes, pharmaco-metrics, and kinetic metrics are included. For kinetic metrics ranges are determined by modeling population growth using 24 different estimated growth models, as described in Figure 1 and Supplemental Figure 1.

Supplementary Dataset 2 – Combination drug screen. Full raw data associated with the combination drug screen described in Figure 3. For all drugs and drug combinations, data are included for cell numbers and lethal fractions at end point, and raw SYTOX fluorescence values over time.

Supplementary Dataset 3 – PCA scores for drugs and drug combinations. For all drugs and drug combinations tested in this study, PCA coefficients for PCs 1-10, as in Figure 5.

Supplementary Dataset 4 – SAD combinations in U2OS cells. 130 SAD combinations in U2OS. Data included for combination name, dominant drug within the combination, Euclidean distance between dominant drug and combination, and Chou-Talalay Combination Index.